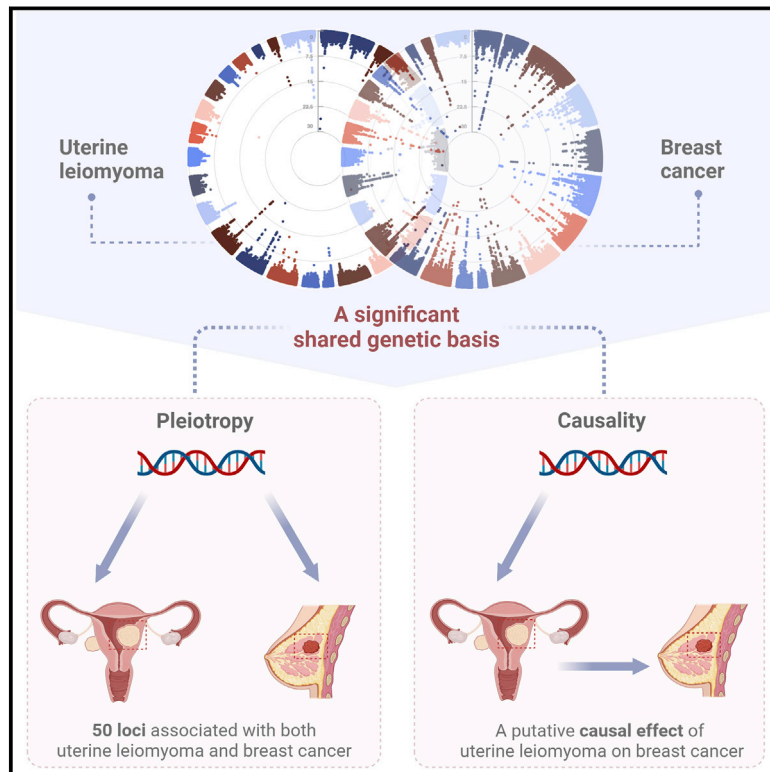


Investigating the shared genetic architecture of uterine leiomyoma and breast cancer: A genome-wide cross-trait analysis

Graphical abstract



Authors

Xueyao Wu, Chenghan Xiao,
Zhitong Han, ...,
Cynthia Casson Morton, Jiayuan Li,
Xia Jiang

Correspondence

lijayuan73@163.com (J.L.),
xiajiang@scu.edu.cn (X.J.)

Wu et al. demonstrate a significant shared genetic basis, multiple pleiotropic loci, as well as a putative causal relationship between uterine leiomyoma and breast cancer, highlighting a biological link underlying these two complex female diseases. These findings provide important implications for future therapeutic strategy and risk prediction.



Investigating the shared genetic architecture of uterine leiomyoma and breast cancer: A genome-wide cross-trait analysis

Xueyao Wu,¹ Chenghan Xiao,¹ Zhitong Han,² Li Zhang,¹ Xunying Zhao,¹ Yu Hao,¹ Jinyu Xiao,¹ C. Scott Gallagher,³ Peter Kraft,^{4,5} Cynthia Casson Morton,^{6,7,8,9,12} Jiayuan Li,^{1,12,*} and Xia Jiang^{1,10,11,12,*}

Summary

Little is known regarding the shared genetic architecture or causality underlying the phenotypic association observed for uterine leiomyoma (UL) and breast cancer (BC). Leveraging summary statistics from the hitherto largest genome-wide association study (GWAS) conducted in each trait, we investigated the genetic overlap and causal associations of UL with BC overall, as well as with its subtypes defined by the status of estrogen receptor (ER). We observed a positive genetic correlation between UL and BC overall ($r_g = 0.09$, $p = 6.00 \times 10^{-3}$), which was consistent in ER+ subtype ($r_g = 0.06$, $p = 0.01$) but not in ER- subtype ($r_g = 0.06$, $p = 0.08$). Partitioning the whole genome into 1,703 independent regions, local genetic correlation was identified at 22q13.1 for UL with BC overall and with ER+ subtype. Significant genetic correlation was further discovered in 9 out of 14 functional categories, with the highest estimates observed in coding, H3K9ac, and repressed regions. Cross-trait meta-analysis identified 9 novel loci shared between UL and BC. Mendelian randomization demonstrated a significantly increased risk of BC overall (OR = 1.09, 95% CI = 1.01–1.18) and ER+ subtype (OR = 1.09, 95% CI = 1.01–1.17) for genetic liability to UL. No reverse causality was found. Our comprehensive genome-wide cross-trait analysis demonstrates a shared genetic basis, pleiotropic loci, as well as a putative causal relationship between UL and BC, highlighting an intrinsic link underlying these two complex female diseases.

Introduction

Uterine leiomyoma (UL), also known as fibroids, are benign tumors affecting 5.4%–77.0% of women of reproductive age.¹ Although the majority of UL are asymptomatic, nearly 25% of women with UL may experience heavy menstrual bleeding, abdominal pain, infertility, and increased risk of miscarriage.² Breast cancer (BC), on the other hand, affects 1 in 10 women throughout their lifetimes and ranks first in both incidence and mortality of female cancers.³ A shared etiology underlying these two complex diseases has long been recognized. Several common risk factors including obesity, oral contraceptive use, hormone replacement therapy, and reproductive factors may lead to increased levels of estrogen and progesterone.^{4,5} Furthermore, epidemiological studies have evaluated and largely demonstrated a UL-BC phenotypic link. Leveraging data from 2,411 BC-affected individuals and the entire registered female population (aged 20 years or above, $N = 162,449$) of Gothenburg, Sweden, Lindegård et al. found a significantly increased risk of UL associated with non-fatal BC (observed/expected BC cases = 1.7,

$p < 0.01$).⁶ Later on, a prospective cohort study of 57,747 African American women reported a non-significant but positive association for early-diagnosed UL with BC before age 40 (IRR = 1.39, 95% CI = 0.97–1.99).⁷ With a two-times augmented sample size and a median follow-up time of 6.5 years, Shen et al. found a 31% increased risk of BC in women diagnosed with UL compared to UL-free referents of East Asian ancestry (HR = 1.31, 95% CI = 1.13–1.52).⁸ Nevertheless, owing to the observational nature of conventional epidemiological studies, phenotypic correlations derived from these studies are likely subject to bias, confounding, and reverse causality.⁹

Linking traits through genetics overcomes at least one major challenge of observational studies—reverse causality—and with careful design can also address confounding. Indeed, current progress from genome-wide association studies (GWASs) have elucidated a considerable number of disease-associated variants (single nucleotide polymorphisms, SNPs) for both UL ($n = 29$) and BC ($n > 150$).^{10,11} The SNP heritability of UL and BC has further been quantified as 3%–13%^{10,12} and 13%–18%,^{11,13} respectively, indicating a non-trivial genetic

¹Department of Epidemiology and Health Statistics, West China School of Public Health and West China Fourth Hospital, Sichuan University, Chengdu, Sichuan 610041, China; ²Department of Life Sciences, Sichuan University, Chengdu, Sichuan 610041, China; ³Department of Genetics, Harvard Medical School, Boston, MA 02115, USA; ⁴Department of Biostatistics, Harvard T.H. Chan School of Public Health, Boston, MA, USA; ⁵Department of Epidemiology, Harvard T.H. Chan School of Public Health, Boston, MA, USA; ⁶Department of Obstetrics and Gynecology, Brigham and Women's Hospital, Harvard Medical School, Boston, MA 02115, USA; ⁷Department of Pathology, Brigham and Women's Hospital, Harvard Medical School, Boston, MA 02115, USA; ⁸Broad Institute of MIT and Harvard, Cambridge, MA 02142, USA; ⁹Manchester Centre for Audiology and Deafness, Manchester Academic Health Science Center, University of Manchester, Manchester M13 9PL, UK; ¹⁰Department of Clinical Neuroscience, Center for Molecular Medicine, Karolinska Institutet, Solna, Stockholm, Sweden; ¹¹Program in Genetic Epidemiology and Statistical Genetics, Harvard T. H. Chan School of Public Health, Boston, MA, USA

¹²These authors contributed equally to this work

*Correspondence: lijayuan73@163.com (J.L.), xiajiang@scu.edu.cn (X.J.)

<https://doi.org/10.1016/j.ajhg.2022.05.015>

© 2022 American Society of Human Genetics.



component in disease susceptibility. Multiple loci (i.e., *GREB1*, *NEK10*, *TERT*, *ESR1*, *TP53*, and *MCM8*) influencing both traits have also been identified,^{10,12} suggesting the observed epidemiological association is at least in part attributable to a shared genetic architecture.

The accumulating amount of genome-wide genetic data enable the utilization of a recently developed statistical genetics tool, named genome-wide cross-trait analysis. This design offers an unprecedented opportunity to characterize comprehensively the shared genetic architecture and causal link across traits, driving forward epidemiologic associations with novel insights into the underlying biological mechanisms.⁹ Such analysis has several analytic aspects: a genetic correlation analysis to estimate global and local genetic correlation, a cross-trait meta-analysis to identify shared loci, and Mendelian randomization (MR) to make causal inference. Nevertheless, to the best of our knowledge, no genome-wide cross-trait analysis has been conducted to explore systematically the shared and distinct etiology underpinning UL and BC.

Therefore, in this study, we performed a comprehensive genome-wide cross-trait analysis to investigate the genetic overlap as well as the causal relationship underlying UL and BC. First, we quantified genetic correlation to understand shared genetic basis. Next, we applied cross-trait meta-analysis to identify pleiotropic loci, of which biological function was further annotated, leveraging information from high-quality functional resources. Finally, we performed a bidirectional two-sample MR analysis to infer putative causal relationships. The overall study design is shown in [Figure 1](#).

Material and methods

Data summary

This is a secondary analysis of existing GWASs. Summary statistics were retrieved from publicly available GWASs conducted for UL and BC. Details on the characteristics of each included dataset are presented in [Table S1](#).

Uterine leiomyoma

The latest GWAS of UL was performed by Gallagher et al. in 2019,¹⁰ meta-analyzing data from five participating cohorts of the FibroGENE consortium (Women's Genome Health Study [WGHS], Northern Finnish Birth Cohort [NFBC], QIMR Berghofer Medical Research Institute [QIMR], UK Biobank [UKB], and 23andMe). This GWAS combined 8.7 million variants in 35,474 UL-affected women and 267,505 female control subjects (all of European ancestry). UL was determined based on either self-report or clinical documentation. SNPs were imputed to the 1000 Genomes Project (1KGP) Phase 3 reference panel or the Haplo-type Reference Consortium (HRC) reference panel. A fixed-effect inverse-variance-weighted meta-analysis was conducted across all cohorts. Top-associated SNPs in the combined meta-analysis reaching a p threshold of 5×10^{-8} were reported.

We extracted relevant information of the 29 GWAS-identified UL-associated significant SNPs and used those SNPs as instru-

mental variables (IVs). Details on the characteristics of UL-associated IVs are shown in [Table S2](#). We also retrieved full set summary statistics of UL.

Breast cancer

For BC overall, the most recent also the largest GWAS was performed by Zhang et al. in 2020,¹¹ meta-analyzing data from 82 participating studies of the Breast Cancer Association Consortium (BCAC) and 11 other BC genetic studies. This GWAS combined 10.8 million variants in 133,384 BC-affected women and 113,789 female control subjects (all of European ancestry). SNPs were imputed to the 1KGP Phase 3 reference panel. A fixed-effect inverse-variance-weighted meta-analysis was conducted across all studies. Top-associated SNPs in the combined meta-analysis reaching a p threshold of 5×10^{-8} were reported. This GWAS confirmed 153 previous-reported BC SNPs and additionally identified 32 novel BC SNPs, for a total of 185 SNPs.

For subtype-specific BC, we retrieved summary statistics from the largest published GWAS on estrogen receptor (ER)+ and ER-BC performed by Michailidou et al. in 2017.¹³ This GWAS meta-analyzed data from BCAC and DRIVE (Discovery, Biology and Risk of Inherited Variants in Breast Cancer Consortium), combining 11.8 million variants in 122,977 BC-affected women (of which 69,501 were ER+ cases and 21,468 were ER-) and 105,974 female control subjects (all of European ancestry). Data imputed to the 1KGP reference panel were analyzed using a fixed-effects inverse-variance-weighted meta-analysis.

From both GWASs, we extracted effect sizes and relevant information for the 29 UL-associated IVs. We also extracted relevant information of the 185 GWAS-identified BC-associated significant SNPs (characteristics of which are shown in [Table S3](#)) and retrieved full set summary statistics of BC.

Statistical analysis

Global genetic correlation analysis

To evaluate a shared genetic basis between UL and BC, we performed a global genetic correlation analysis using linkage disequilibrium (LD) score regression (LDSC).¹⁴ LDSC estimates genetic correlation (r_g) (ranging from -1 to 1) using only summary statistics, relying on the fact that GWAS effect size estimate for a given variant includes the effects of all variants in LD with that variant, which can be extended to the analysis of genetic correlation between traits if the χ^2 statistics are replaced with the product of two z-scores from traits of interest. More precisely, by implementing the algorithms described below, LDSC uses the slope from the regression of z-scores on LD-score to estimate r_g :

$$E[z_{1j}z_{2j}l_j] = \frac{\sqrt{N_1N_2}\rho_g l_j}{M} + \frac{N_s\rho}{\sqrt{N_1N_2}}$$

$$r_g = \rho_g / \sqrt{h_1^2 h_2^2}$$

where z_{1j} and z_{2j} are the z-scores of SNP j from trait 1 and trait 2, r_g N_1 and N_2 are the sample sizes for trait 1 and trait 2, ρ_g is the genetic covariance, l_j is the LD-score, M is number of SNPs, N_s is the number of overlapping samples, ρ is the phenotypic correlation in overlapping samples, and h_1^2 and h_2^2 are the SNP heritability of trait 1 and trait 2.

LDSC analysis was performed using the known LD structure of European ancestry reference data from 1KGP and was restricted to only HapMap3 SNPs, recognized as well imputed in most studies to minimize bias due to low imputation quality. We

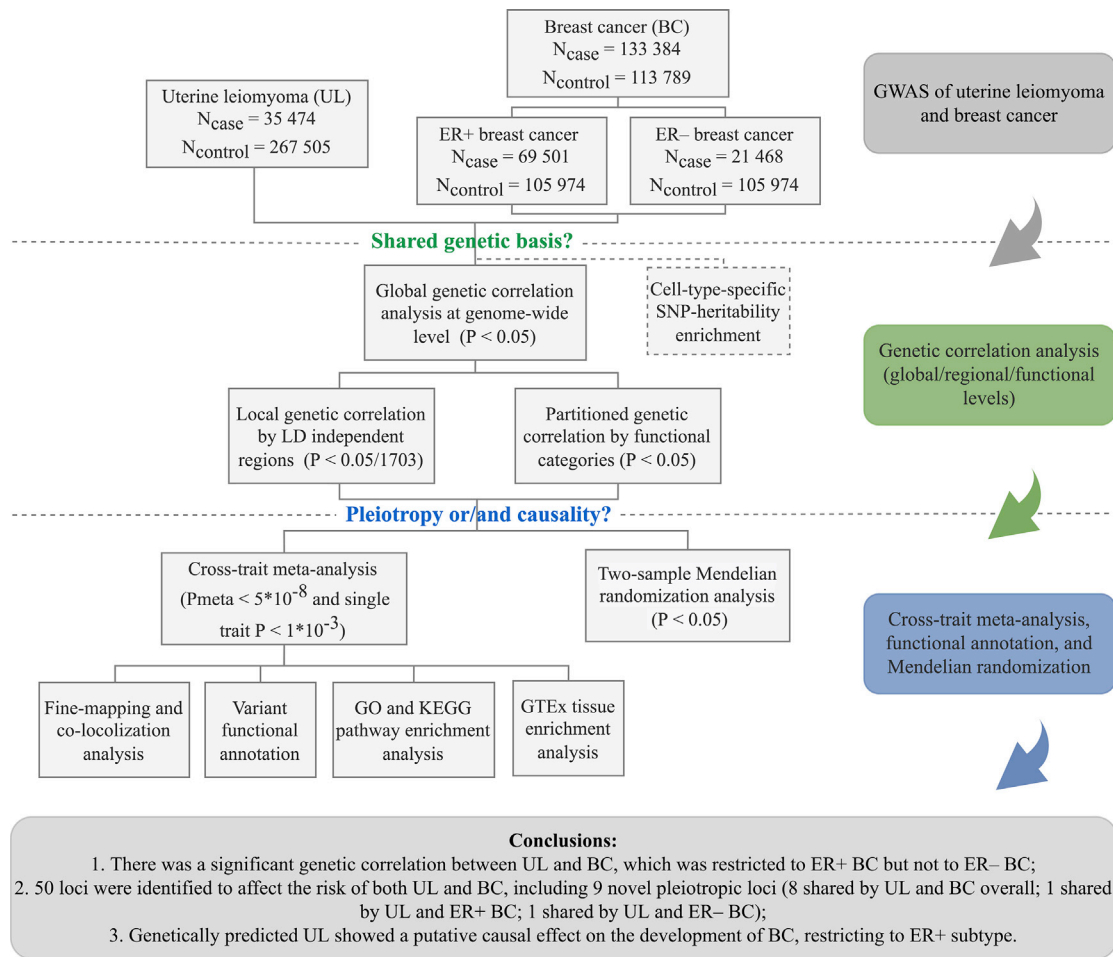


Figure 1. Overall study design of genome-wide cross-trait analysis

GWAS summary statistics for each trait of interest were retrieved from publicly available GWASs. A global genetic correlation analysis between uterine leiomyoma and breast cancer was conducted. The estimated global genetic correlation was further dissected at LD-defined regions and by functional categories. Cross-trait meta-analysis was applied to identify pleiotropic loci, and a bidirectional two-sample Mendelian randomization analysis was used to infer putative causal relationship. UL, uterine leiomyoma; BC, breast cancer; ER, estrogen receptor; GTEx, Genotype-Tissue Expression project; GWAS, genome-wide association study.

conducted LDSC with and without a constrained intercept, as constraining the single-trait heritability intercept increases the accuracy of estimation when sample overlap and population stratification are minimal.¹⁴ A false discovery rate (FDR) corrected p value (Benjamin-Hochberg procedure) of 0.05 was used as significant threshold (FDR $p < 0.05$).

Local genetic correlation analysis

Global genetic correlations estimated by LDSC are based on aggregated information across all variants in the genome. It is possible that even though two traits are of negligible global genetic correlation, there are specific regions in the genome contributing to both traits. Therefore, we further calculated pairwise local genetic correlations for UL and BC using ρ -HESS.¹⁵ ρ -HESS provides a precise quantification of the similarity between pairs of traits driven by genetic variations at each specific region in the genome, using approximately 1,703 independent LD blocks with an average length of 1.6 Mb. Bonferroni correction was applied to adjust for multiple testing (two-tailed $p < 0.05/1,703$).¹⁵

Partitioned genetic correlation analysis

To investigate the contribution of genomic functional elements, we further partitioned the global UL-BC genetic correlation using stratified-LDSC.¹⁶ Fourteen functional categories were used: cod-

ing region, conserved region, DNase digital genomic foot-printing (DGF) region, DNase I hypersensitive sites (DHSs), fetal DHS, intronic region, promotor, repressed region, super-enhancer, transcribed region, and histone marks H3K27ac, H3K4me1, H3K4me3, and H3K9ac. Stratified-LDSC partitions SNPs into different functional categories and calculates LD-score for each given SNP to that category, which were used to estimate genetic correlation within that specific functional category.

Cross-trait meta-analysis

Shared genetic components suggest either genetic variants having independent effect on both traits (pleiotropy) or genetic variants influencing one trait via its effect on the other (causality). We next performed a cross-trait meta-analysis using Cross-Phenotype Association (CPASSOC)¹⁷ to identify pleiotropic loci. Using summary statistics of single SNP-trait associations from GWAS, CPASSOC provides two estimates, S_{Hom} and S_{Het} . S_{Hom} is based on a fixed-effect meta-analysis approach and can be viewed as the maximum of weighted sum of trait-specific genetic effects. It is less powerful under the presence of between-study heterogeneity, which is common when meta-analyzing multiple traits. As an extension of S_{Hom} , S_{Het} maintains statistical power even under the presence of heterogeneity by assigning more weights to the larger

trait-specific effect sizes. This method (S_{Het}) was thus adopted for the analysis herein.

Independent loci were obtained using the PLINK¹⁸ “clumping” function through applying the following parameters: $-\text{clump-p1 } 5\text{e-}8$ $-\text{clump-p2 } 1\text{e-}5$ $-\text{clump-r2 } 0.2$ $-\text{clump-kb } 500$. Within each locus, the variant with the lowest p value was kept as the index SNP. Significant pleiotropic SNPs were defined as index variants satisfying $P_{\text{CPASSOC}} < 5 \times 10^{-8}$ and $p_{\text{single-trait}} < 1 \times 10^{-3}$ (for both traits). SNPs that were not identified as significant by the original single-trait GWASs, meaning they themselves were independent ($r^2 < 0.20$) of those previously reported genome-wide significant SNPs (of BC and UL), and none of their neighboring SNPs within 1.0 Mb region reached $p < 5 \times 10^{-8}$ in the single-trait GWAS (of BC and UL), were considered as novel pleiotropic SNPs and were prioritized in this study.

We used Ensemble Variant Effect Predictor (VEP)¹⁹ and 3DSNP²⁰ for detailed functional annotation of the identified pleiotropic SNPs.

Fine mapping credible set analysis

The index SNP does not necessarily indicate the causal SNP.²¹ We further identified a credible set of variants that were 99% likely, based on posterior probability, to contain causal variants at each of the pleiotropic loci using FM-summary.²² Briefly, FM-summary is a Bayesian fine-mapping algorithm that maps only the primary signal and uses a flat prior with steepest descent approximation, assuming at least one causal variant exists within a given region.

Colocalization analysis

Another approach to understanding the shared genetic basis cross traits is to investigate whether the same variants are responsible for two GWAS signals or whether it is distinct genetic variants close to each other. We next performed a colocalization analysis through Coloc.²³ Coloc uses a Bayesian algorithm to generate posterior probabilities for five mutually exclusive hypotheses regarding the sharing of causal variants in a genomic region, namely H_0 (no association), H_1 or H_2 (association to one trait only), H_3 (association to both traits, two distinct SNPs), and H_4 (association to both traits, one shared SNP). We extracted summary statistics for variants within 1.0 Mb of the index SNP at each shared locus and calculated the posterior probability for H_4 (PPH4) and H_3 (PPH3). A locus was considered colocalized if PPH4 or PPH3 was greater than 0.5.

Pathway and GTEx tissue enrichment analysis

To gain biological insights for the novel pleiotropic SNPs identified from CPASSOC, we performed post-GWAS functional annotation by leveraging multiple resources. We applied the WebGestalt tool²⁴ to assess the enrichment of novel shared genes in Gene Ontology (GO) biological processes and Kyoto Encyclopedia of Genes and Genomes (KEGG) pathways. To identify tissues most relevant to the shared genes, we performed GTEx tissue enrichment analysis using functional mapping and annotation of genome-wide association studies (FUMA)²⁵ GENE2FUNC process with 54 tissue types available from GTEx (v.8). The Benjamin-Hochberg procedure was used to correct for multiple testing.

Cell-type-specific enrichment of SNP heritability

To understand further the (dis)similarity across traits, we partitioned heritability using stratified-LDSC leveraging genome-wide genetic variants of UL and BC. We used 396 annotations constructed by the Roadmap project for six chromatin marks (DHS, H3K27ac, H3K36me3, H3K4me1, H3K4me3, and H3K9ac) in a set of 88 primary cell types or tissues. Each cell-type-specific annotation corresponded to a chromatin mark in a single cell type, and there were 396 such annotations in total. We further divided these

396 cell-type-specific annotations into 9 broad groups, namely adipose, central nervous system, digestive system, cardiovascular, musculoskeletal and connective tissue, immune and blood, liver, pancreas, and other.²⁶ Annotation-specific enrichment values for each trait were calculated using LDSC and were transformed into color scale and visualized by hierarchical clustering. FDR-adjusted p value was applied based on the specific numbers of comparisons made in each analysis.

Mendelian randomization analysis

We finally performed a bidirectional two-sample MR analysis to detect a putative causal relationship. The inverse-variance weighted (IVW) approach was applied as our primary approach.²⁷ This method pools the Wald ratio estimate of each SNP, obtained from dividing the SNP-outcome estimate by the SNP-exposure estimate, using a random-effects inverse-variance method that weights each ratio based on its standard error, and obtains the average casual effect estimates between two traits. Complementary to IVW, we also adopted MR-Egger regression and weighted median approach. MR-Egger regression can be used to detect and correct for bias due to directional pleiotropy.²⁸ Weighted median approach provides a consistent estimate of the causal effect even when up to 50% of genetic variants are invalid.²⁹ These two approaches were less powerful than IVW in detecting true causal effects and were therefore used to complement with findings from IVW. A causal estimate was considered significant if it was significant in IVW and showed directional consistency in MR-Egger regression and weighted median approach.

To validate MR model assumptions, that the IVs (1) are strongly associated with the exposure, (2) share no common cause with the outcome, and (3) affect the outcome only through the exposure,³⁰ we conducted several important sensitivity analyses. First, we excluded palindromic IVs, SNPs whose alleles are represented by the same pair of nucleotides on the forward and the reverse strands, introducing ambiguity into the identification of effect allele. Second, we excluded pleiotropic SNPs which were associated with potential confounding phenotypes according to the GWAS catalog. Third, we performed leave-one-out analysis where one SNP was removed at a time and IVW was conducted based on the remaining SNPs. Finally, MR-Pleiotropy Residual Sum and Outlier (MR-PRESSO) method³¹ was applied to detect and correct for horizontal pleiotropy. To adjust for potential confounding effect acting in particular through body mass index (BMI), a risk factor known to influence both UL and BC,^{4,5} we also employed a multi-variable MR.³² To evaluate whether genetic liability to BC exerts a causal effect on UL, we conducted a reverse-direction MR where BC-associated independent SNPs were used as IVs.

Results

Global genetic correlation

Using unconstrained LDSC, a limited genetic correlation was found for UL with BC overall at marginal significance ($r_g = 0.07$, $p = 0.05$). The estimate attenuated to null in BC subtypes (ER+: $r_g = 0.04$, $p = 0.35$; ER-: $r_g = 0.05$, $p = 0.28$). Considering the negligible sample overlap shared by UL and BC, we further constrained the intercepts of genetic covariance estimates to zero, through which LDSC could show greater power with slightly reduced standard errors. As a result, a significant positive genetic correlation was found for UL with BC overall ($r_g = 0.09$,

Table 1. Genome-wide genetic correlations between uterine leiomyoma and breast cancer using constrained and unconstrained LDSC

Trait 1	Trait 2	Constrained LDSC			Unconstrained LDSC		
		r_g	r_{g_SE}	p	r_g	r_{g_SE}	p
Uterine leiomyoma	Breast cancer overall	0.09	0.03	6.00×10^{-3}	0.07	0.04	5.01×10^{-2}
Uterine leiomyoma	ER+ breast cancer	0.06	0.03	1.00×10^{-2}	0.04	0.04	0.35
Uterine leiomyoma	ER- breast cancer	0.06	0.04	0.08	0.05	0.05	0.28

r_g , genetic correlation; SE, standard error; ER, estrogen receptor.

$p = 6.00 \times 10^{-3}$), which, when extended to BC subtypes, remained significant for ER+ subtype ($r_g = 0.06$, $p = 0.01$, withstood multiple correction) but not for ER- subtype ($r_g = 0.06$, $p = 0.08$) (Table 1).

Local genetic correlation

Given the significant global genetic correlation, we further explored whether specific genomic regions conferred local genetic correlation (Figure 2, Tables S4–S6). After multiple correction, a strong local signal was found at 22q13.1 (chromosome 22: 39,307,894–40,545,797) for UL with both BC overall ($p = 8.88 \times 10^{-7}$) and ER+ subtype ($p = 4.19 \times 10^{-6}$). This genomic region harbors *TNRC6B*, a contributor to tumorigenesis of different cancers,³³ and *CBX7*, associated with poor prognosis in ovarian clear cell adenocarcinoma.³⁴ We did not observe any additional region that showed significant local genetic correlation.

Partitioned genetic correlation

To characterize genetic overlap at the level of functional categories, we partitioned genetic correlation by 14 functional groups (Figure 3, Table S7). UL was significantly correlated with BC overall at 9 out of 14 functional categories, with r_g ranging from 0.08 (H3K27ac) to 0.15 (coding). The repressed region ($r_g = 0.14$), H3K9ac ($r_g = 0.12$), and promotor region ($r_g = 0.11$) also showed strong genetic correlation. Looking into BC subtypes, UL was significantly associated with ER+ BC at 6 functional categories. In addition to coding ($r_g = 0.16$), H3K9ac showed the second strongest genetic correlation ($r_g = 0.13$). For UL and ER- BC, no significant result was identified at any of these functional groups.

Cross-trait meta-analysis and pleiotropic loci

Based on evidence of significant genetic overlap between UL and BC, we next interrogated at individual variant level to identify pleiotropic loci. A total of 8,170,973, 8,175,419, and 8,175,424 SNPs common between UL and BC overall, ER+ BC, and ER- BC were included in the cross-trait meta-analysis, respectively. As a result, 50 independent loci reached genome-wide significance in CPASSOC (fulfilling $p_{CPASSOC} < 5 \times 10^{-8}$ and $p_{single-trait} < 1 \times 10^{-3}$), including 29 loci shared between UL and BC overall, 17 loci shared between UL and ER+ BC, and 14 loci shared between UL and ER- BC (Tables S8–S10). Among these shared loci, those closest to well-known oncogenes such as *TERT*, *TNRC6B*, and *TP53* showed the strongest signals (i.e., in-

dex SNPs: rs10069690, rs2242652, rs4821942, and rs78378222).

After excluding SNPs that were in LD ($r^2 \geq 0.20$) with any of the previously reported single-trait-associated significant SNPs, we identified 8 novel pleiotropic SNPs for UL and BC overall of which 1 was also shared by UL and ER+ BC, and 1 novel pleiotropic SNP for UL and ER- BC, totaling 9 newly discovered SNPs (Table 2). Notably, rs3176337 ($p_{CPASSOC} = 7.87 \times 10^{-11}$), the most significant novel SNP shared by UL and BC overall, was also identified as a novel pleiotropic SNP for UL and ER+ BC. This locus was near *CDKN1A*, a gene encoding a cyclin-dependent kinase inhibitor, which is a pivotal cell cycle regulator ensuring genomic stability and is often deregulated in human cancer.³⁵ The second most significant novel SNP was mapped to *PTPN11* (rs11066320, $p_{CPASSOC} = 1.31 \times 10^{-9}$). *PTPN11* is a member of the protein tyrosine phosphatase family, involved in a variety of cellular processes including cell growth, differentiation, mitotic cycle, and oncogenic transformation.³⁶ Index SNP rs35840638 implicating *ADAP2* was the third strongest shared signal ($p_{CPASSOC} = 2.17 \times 10^{-9}$), specifically shared by UL and ER- BC. The fourth strongest signal was in close proximity to an intergenic region closest to *GSTM1* (rs4147562, $p_{CPASSOC} = 2.83 \times 10^{-9}$), which encodes a glutathione S-transferase that belongs to the mu class, and functions in the detoxification of electrophilic compounds such as products of oxidative stress and carcinogens.³⁷ Other novel shared genetic variants were rs13001657 (intergenic region), rs62408878 (*GNB4*, *MFN1*), rs9316500 (*DLEU1*, *RP11-175B12.2*), rs3790110 (*GNAO1*), and rs2281925 (*SLC2A4RG*, *ZBTB46*), including regions previously implicated in energy metabolism and multiple cell cycle processes.^{38–41} Detailed annotation for each SNP discovered by cross-trait meta-analysis is shown in Table S11.

Identification of causal variants and colocalization

Fine-mapping analysis assessed the 99% credible set of causal variants at each of the CPASSOC-identified pleiotropic loci, providing targets for downstream experimental analysis (results shown in Tables S12–S14). In general, we identified 138 candidate causal SNPs for novel shared loci between UL and BC overall, numbers specific to each index SNP were: rs4147562 (2), rs13001657 (23), rs62408878 (1), rs3176337 (5), rs11066320 (7), rs9316500 (11), rs3790110 (80), and rs2281925 (9). For novel loci shared between UL

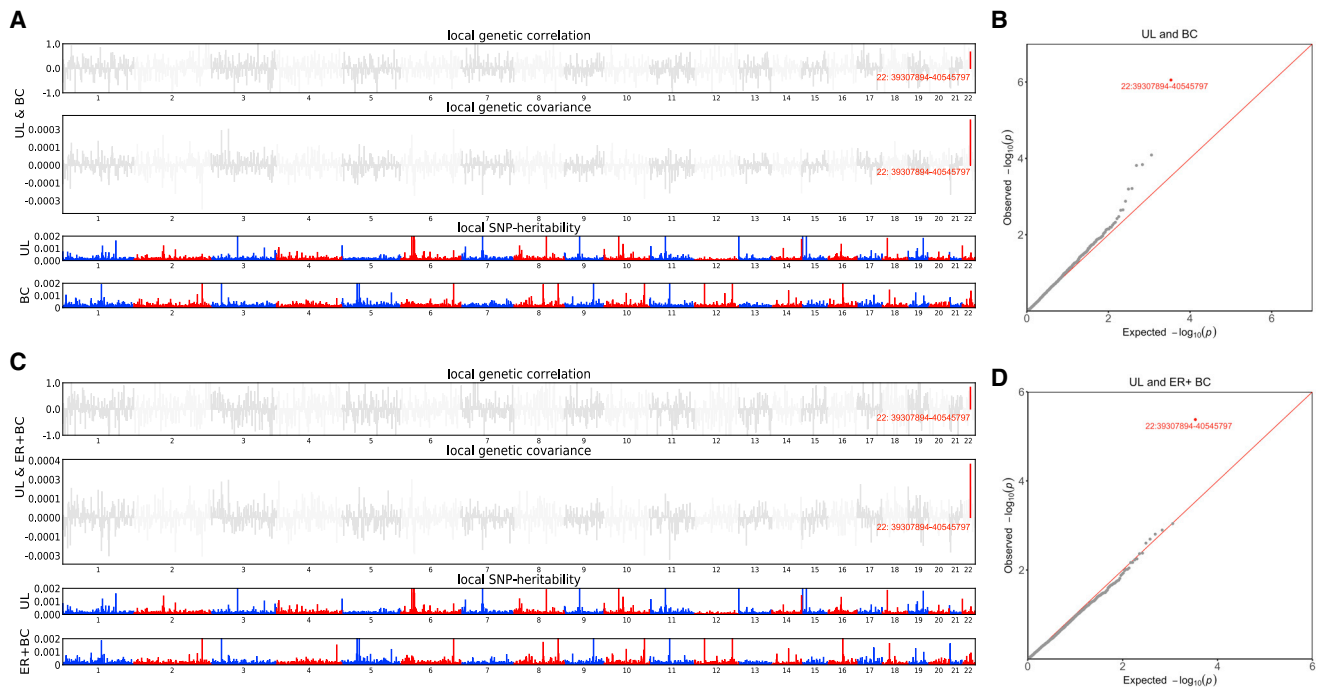


Figure 2. Local genetic correlation between uterine leiomyoma and breast cancer

(A) Manhattan plot showing the estimates of local genetic correlation, genetic covariance, and SNP heritability between uterine leiomyoma and breast cancer overall. Red bars represent loci showing significant local genetic correlation after multiple testing adjustment ($p < 0.05/1,703$).

(B) QQ-plot presenting region-specific p values from local genetic correlation between uterine leiomyoma and breast cancer overall.

(C) Manhattan plot showing the estimates of local genetic correlation, genetic covariance, and SNP heritability between uterine leiomyoma and ER+ breast cancer. Red bars represent loci showing significant local genetic correlation after multiple testing adjustment ($p < 0.05/1,703$).

(D) QQ-plot presenting region-specific p values from local genetic correlation between uterine leiomyoma and ER+ breast cancer. UL, uterine leiomyoma; BC, breast cancer; ER, estrogen receptor.

and BC subtypes, 17 and 13 candidate causal SNPs were discovered for rs3176337 and rs35840638, respectively.

Colocalization analysis was further performed to determine whether the genetic variants driving the association in two traits are the same or different. Most shared loci between UL and BC colocalized at the same candidate causal SNPs ($PPH4 > 0.5$) (22/50) or at different candidate causal SNPs ($PPH3 > 0.5$) (16/50), reinforcing shared causal associations (Table S15). Among the 9 novel pleiotropic loci, 2 loci (index SNP: rs11066320 and rs35840638) showed evidence of colocalization ($PPH4 > 0.5$).

Biological pathway, GTEx tissue, and SNP-heritability enrichment

After multiple correction, GO analysis across the 9 novel pleiotropic loci revealed enrichment in the benzene-containing compound metabolic process (GO:0042537, $p = 9.87 \times 10^{-06}$). KEGG analysis further identified significant enrichment in platinum drug resistance (hsa01524, $p = 7.91 \times 10^{-06}$). In GTEx tissue enrichment analysis, heart left ventricle was identified to be significantly enriched for the expression of novel shared genes underlying UL and BC (Figure S1). Results using all pleiotropic loci are shown in Tables S16 and S17 and Figure S2.

Partitioning SNP heritability by using 396 cell-type-specific annotations, we identified FDR-significant heritability enrichment for UL in smooth muscle and cardiovascular system (i.e., fetal heart, aorta, and right atrium). Although no significant enrichment was observed for BC overall or BC subtypes, they clustered closely with UL at each chromatin mark in musculoskeletal and connective, cardiovascular and digestive system, as well as other tissues or cell types such as ovary, obesity, mammary epithelial cells, fetal kidney, and primary B cells. Interestingly, different clustering patterns were observed comparing cell-type-specific enrichment for UL with ER+ versus ER- BC, where both UL and ER+ subtype were enriched for certain annotations while ER- subtype was not, for example, pancreas, fetal lung, and certain blood/immune system-related components (Figure S3).

Mendelian randomization

We finally conducted a two-sample MR using 28 GWAS-identified UL-associated SNPs as IVs (one SNP, rs2456181, was not available in the outcome GWASs). F -statistics for these IVs was 804.14, suggesting strong instruments (Tables S2 and S3). Using IVW, genetic liability to UL was significantly associated with an increased risk of BC overall (OR = 1.09, 95%CI = 1.01–1.18, $p = 0.03$). The

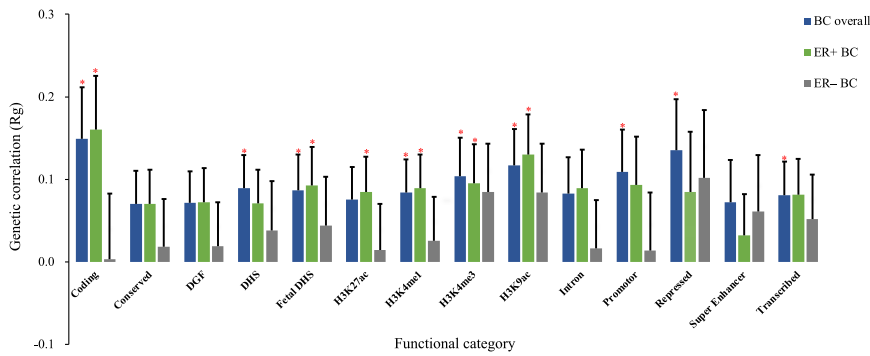


Figure 3. Partitioned genetic correlation between uterine leiomyoma and breast cancer by genomic functional elements
Vertical axis represents genetic correlation. Horizontal axis represents 14 functional categories. Asterisks represent significance ($p < 0.05$), error bars represent the standard error of genetic correlation. UL, uterine leiomyoma; BC, breast cancer; ER, estrogen receptor; DGF, DNase digital genomic footprinting; DHS, DNase I hypersensitive sites.

estimates remained directionally consistent in MR-Egger regression and weighted median approach, despite larger statistical uncertainties. No sign of horizontal pleiotropy was detected ($p_{\text{MR-Egger intercept}} = 0.45$). Subgroup analysis further identified such an association to be restricted to ER+ subtype (IVW OR = 1.09, 95%CI = 1.01–1.17, $p = 0.03$; $p_{\text{MR-Egger intercept}} = 0.94$) but not to ER- subtype (IVW OR = 1.05, 95%CI = 0.88–1.25, $p = 0.57$; $p_{\text{MR-Egger intercept}} = 0.05$) (Figure 4).

We performed important sensitivity analysis to verify MR model assumptions. The causal effect of UL in BC overall or ER+ subtype remained significant after excluding palindromic SNPs or pleiotropic SNPs. The leave-one-out analysis demonstrated that the observed causal relationship was not driven by any outlying variant (Figure S4). After removing outliers, MR-PRESSO yielded similar associations (BC overall OR = 1.05, $p = 0.049$; ER+ subtype OR = 1.09, $p = 2.67 \times 10^{-3}$; ER- subtype OR = 1.02, $p = 0.72$) (Figure 4). Multi-variable IVW taking into consideration BMI generated similar results (BC overall OR = 1.10, $p = 0.02$; ER+ subtype OR = 1.10, $p = 0.03$; ER- subtype OR = 1.06, $p = 0.57$), suggesting a causal association of UL with BC independent of obesity.

Using the 185 GWAS-identified BC-associated SNPs as IVs, we performed a reverse-direction MR. No evidence was found on the association between genetic liability to BC and UL risk (IVW OR = 1.00, $p = 0.80$; MR-Egger OR = 1.01, $p = 0.68$; weighted median OR = 1.00, $p = 0.87$) (Figure 4).

Discussion

To the best of our knowledge, this is the first large-scale genome-wide cross-trait analysis that systematically interrogates the shared genetic basis underlying UL and BC, two highly complicated and entangled disorders. We found evidence supporting a significant genetic correlation of UL with BC and with its ER+ subtype. When the whole genome was partitioned, significant correlations were further discovered within a specific genomic region (22q13.1) and functional categories (e.g., coding, H3K9ac, and repressed region). Using cross-trait meta-analysis, we identified multiple pleiotropic loci with joint asso-

ciations. Additionally, MR analysis highlighted a putative causal role of UL on BC risk, restricted to ER+ subtype.

Using LDSC with a constrained intercept, we detected a significant global genetic correlation of UL with BC overall, as well as with ER+ subtype. Constrained LDSC is known for improving the statistical power of r_g estimated under the assumption of no sample overlap¹⁴ and was applied in our study for two reasons. First, the UL and BC GWASs shared no overlapping participating studies, and second, the intercepts of genetic covariance were estimated at around zero (~ 0.001 – 0.007). Both reasons indicate an absence of bias from sample overlap or population stratification, justifying the utilization of the method. Partitioning the whole genome into 1,703 nearly independent regions, we found a strong local genetic correlation of UL at 22q13.1 with both overall and ER+ BC. This region harbors *TNRC6B*, a gene previously reported to be independently associated with UL and BC.^{10–12} In stratified-LDSC, significant genetic correlation was further observed in multiple annotated regions of the genome. The strongest partitioned r_g was found, unsurprisingly, to be in the coding region, while partitioned r_g was also high (or even higher than the global r_g) in certain non-coding regions, including histone acetylation marks (i.e., H3K9ac) and histone modification marks (i.e., H3K4me1 and H3K27me3), highlighting their important roles in not only the progression of BC⁴² but also in the onset of disease. This observation is consistent with the idea that genetic variation within functional non-coding elements is also substantially involved in gene expression and regulation.^{43,44} Unfortunately, and consistently, no significant genetic correlation was observed for UL and ER- BC at any level from global r_g to local r_g .

While our findings demonstrate a putative shared etiology between UL and BC, it can be the result of pleiotropy (a situation in which a genetic variant or gene has effects on multiple traits) and/or causality (a situation in which a genetic variant has an effect on a trait via its genetic effect on an intermediate trait).⁹ In our downstream analysis performed to dissect such a complex genetic relationship, a total of 50 shared loci between UL and BC were identified of which 41 loci were previously reported to be significantly associated with UL and/or BC. These loci harbor genes previously implicated in risks of various carcinomas

Table 2. Novel pleiotropic loci between uterine leiomyoma and breast cancer ($p_{\text{CPASSOC}} < 5 \times 10^{-8}$, $5 \times 10^{-8} < \text{single trait p value} < 1 \times 10^{-3}$)

SNP	Chr: Position	A1/A2	UL		BC		p_{CPASSOC}	Genes within clumping range	Linear closest gene ^a	Interacting gene ^b
			BETA	p	BETA	p				
Uterine leiomyoma and breast cancer overall										
rs4147562	chr1: 110,230,073–110,230,099	A/T	−0.46	2.9×10^{-05}	0.04	3.5×10^{-05}	2.8×10^{-09}	intergenic region	<i>GSTM1</i>	<i>GSTM4</i>
rs13001657	chr2: 88,795,621–89,103,554	A/G	0.04	1.1×10^{-04}	0.03	4.2×10^{-05}	2.2×10^{-08}	<i>ANKRD36BP2</i> , <i>EIF2AK3</i> , <i>LOC101928371</i> , <i>RPIA</i> , <i>TEX37</i>	–	<i>EIF2AK3</i>
rs62408878	chr3: 179,112,234–179,112,234	T/C	0.41	4.3×10^{-06}	−0.03	6.5×10^{-04}	7.3×10^{-09}	intergenic region	<i>GNB4</i> , <i>MFN1</i>	–
rs3176337	chr6: 36,618,140–36,648,920	A/C	0.04	4.8×10^{-06}	−0.03	8.3×10^{-06}	7.9×10^{-11}	<i>CDKN1A</i> , <i>PANDAR</i>	<i>CDKN1A</i>	<i>MIR3925</i>
rs11066320	chr12: 112,486,818–112,906,415	A/G	−0.03	2.2×10^{-04}	−0.03	6.6×10^{-07}	1.3×10^{-09}	<i>HECTD4</i> , <i>MIR6861</i> , <i>NAA25</i> , <i>PTPN11</i> , <i>RPL6</i> , <i>TRAFD1</i>	<i>PTPN11</i>	–
rs9316500	chr13: 51,067,234–51,131,247	T/G	0.03	4.1×10^{-04}	0.03	4.4×10^{-06}	1.3×10^{-08}	<i>DLEU1</i>	<i>DLEU1</i> , <i>RP11-175B12.2</i>	–
rs3790110	chr16: 56,372,907–56,547,254	T/C	−0.03	5.0×10^{-04}	−0.03	6.2×10^{-07}	4.1×10^{-09}	<i>AMFR</i> , <i>BBS2</i> , <i>GNAO1</i> , <i>NUDT21</i> , <i>OGFOD1</i>	<i>GNAO1</i>	<i>CESSA</i>
rs2281925	chr20: 62,318,220–62,376,503	A/G	0.05	3.0×10^{-04}	0.04	2.7×10^{-05}	4.7×10^{-08}	<i>ARFRP1</i> , <i>LIME1</i> , <i>RTEL1</i> , <i>RTEL1-TNFRSF6B</i> , <i>SLC2A4RG</i> , <i>TNFRSF6B</i> , <i>ZBTB46</i> , <i>ZGPAT</i>	<i>SLC2A4RG</i> , <i>ZBTB46</i>	<i>ZGPAT</i>
Uterine leiomyoma and ER+ breast cancer										
rs3176337	chr6: 36,618,140–36,648,920	A/C	0.04	4.8×10^{-06}	−0.03	1.7×10^{-04}	1.5×10^{-08}	<i>CDKN1A</i> , <i>PANDAR</i>	<i>CDKN1A</i>	<i>MIR3925</i>
Uterine leiomyoma and ER− breast cancer										
rs35840638	chr17: 29,166,302–29,318,794	A/G	−0.05	2.3×10^{-07}	−0.05	1.9×10^{-04}	2.2×10^{-09}	<i>ADAP2</i> , <i>ATAD5</i> , <i>DPRXP4</i> , <i>RNF135</i> , <i>TEFM</i>	<i>ADAP2</i>	<i>MIR4724</i>

Position is under build 37 (hg19). SNP, single nucleotide polymorphism; Chr, chromosome; UL, uterine leiomyoma; BC, breast cancer; ER, estrogen receptor.
^aLinear closest genes of index SNPs were mapped by using VEP.
^b3D interacting genes of index SNPs were mapped by using 3DSNP.

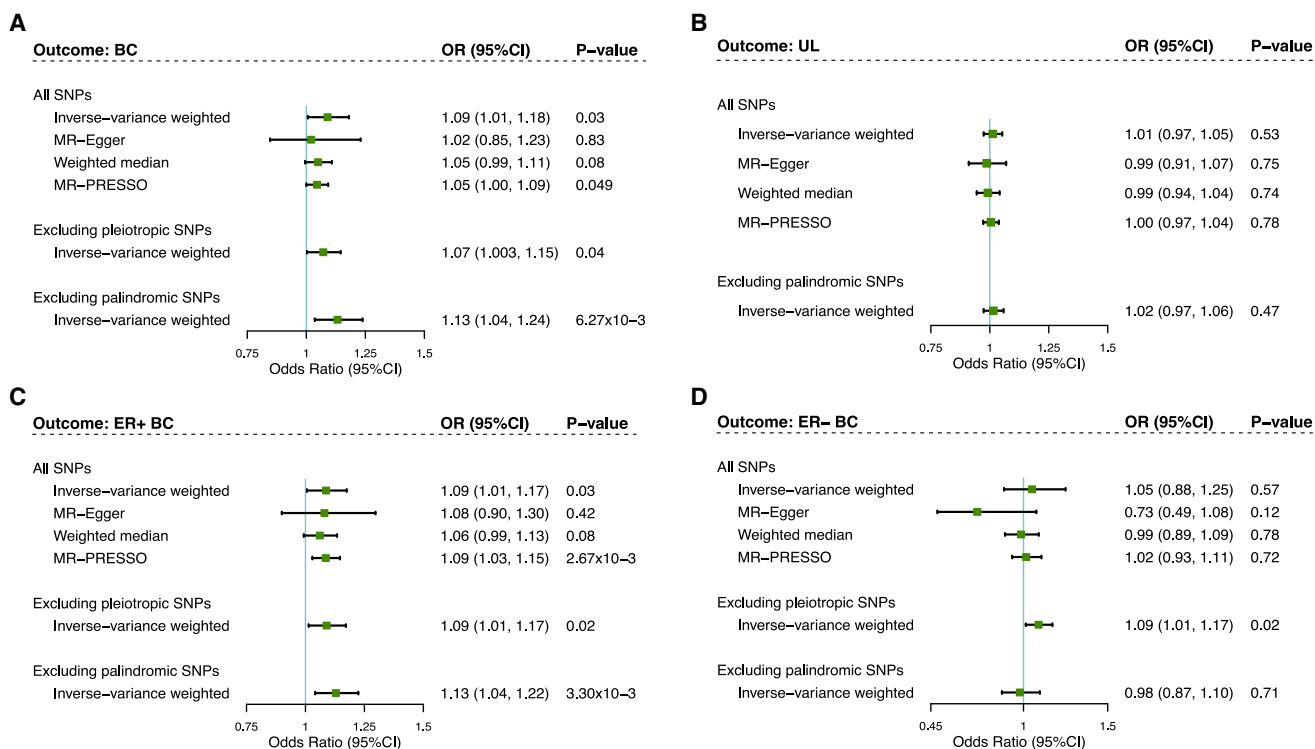


Figure 4. Bidirectional causal relationship underlying uterine leiomyoma and breast cancer

(A) Estimates of causal effect for genetic liability to uterine leiomyoma with breast cancer overall.

(B) Estimates of causal effect for genetic liability to breast cancer overall with uterine leiomyoma.

(C) Estimates of causal effect for genetic liability to uterine leiomyoma with ER+ breast cancer.

(D) Estimates of causal effect for genetic liability to uterine leiomyoma with ER- breast cancer. Boxes represent the point estimates of causal effects, and error bars represent 95% confidence intervals. Inverse-variance weighted approach was adopted as the primary analysis. MR-Egger regression, weighted median, and MR-PRESSO approaches were adopted as sensitivity analysis. UL, uterine leiomyoma; BC, breast cancer; ER, estrogen receptor.

(i.e., *CDKN1A*, *GSTM1*, *MFN1*, *TERT*, *TP53*) or hormone-related traits (i.e., *ESR1*, *GREB1*, and *MCM8*). Multiple genes showed strong evidence of colocalization ($PPH4 > 0.5$), such as *ATAD5*, *EXO1*, *HSPA4*, *MCM8*, *MLLT10*, *PTPN11*, *TERT*, and *TP53*, demonstrating etiological connections. One advantage of meta-analyzing GWASs of different traits is that it improves the statistical power of detecting cross-trait genetic effects (especially for traits with smaller sample sizes) by combining association evidence from multiple GWASs, discovering signals which might not have reached genome-wide significance in a single-trait effort.⁴⁵ Indeed, we found 9 novel loci to be jointly associated with both UL and BC, among which we highlight two interesting examples, *SLC2A4RG/ZBTB46* and *ADAP/MIR4724*.

While *SLC2A4RG* and *ZBTB46* were mapped by the same locus (index SNP: rs2281925), their involvement in breast tumorigenesis has rarely been studied. *SLC2A4RG* is a transcriptional activator of the glucose transporter *SLC2A4*.⁴⁶ Overexpression of *SLC2A4RG* could lead to an inhibition of glioblastoma cell growth by downregulating the expression of cyclin-dependent kinases, suggesting the potential tumor-suppressor role of *SLC2A4RG*.⁴⁷ By performing whole-exome sequencing on paired primary and metastatic tumors, a recent study found *SLC2A4RG* as a signifi-

cantly mutated gene in metastatic BC, despite not reported to play a role in primary BC.⁴⁸ *ZBTB46* is another transcription factor specifically expressed by classical dendritic cells, functioning as a key immune regulator.⁴⁹ Recent studies found *ZBTB46* to be a novel tumor promoter for prostate cancer.^{50,51} Based on microarray expression profile analysis, a study of Chinese women found an upregulated long non-coding RNA, *RP4-583P15.10*, to be differentially expressed between BC tissues and paired adjacent tissues, located downstream of the natural antisense of *ZBTB46*.⁵²

ADAP2 (index SNP: rs35840638) was identified as a significant pleiotropic locus affecting both UL and ER- BC. Furthermore, colocalization analysis showed that this locus had a great probability (98.2%) of containing a shared causal variant of both traits. Using DNA copy number data from 39 cancer types, Maroulis et al. identified *ADAP2* as an essential gene limiting the extent of homozygous deletions in cancer genomes, suggesting its role in the survival of tumor cells.⁵³ In addition, *ADAP2* may be a potential indicator for the early diagnosis and prognosis of acute myeloid leukemia, suggested by Yu et al.⁵⁴ However, there is no result with respect to *ADAP2* function in BC. This locus also interacts with miRNA *MIR4724* in a three-dimensional manner.²⁰ miRNAs are a class of small non-coding RNAs regulating a wide range of physiological processes

by repressing transcription or translation of their target genes, which may contribute to cancer etiology.⁵⁵ *MIR4724* has only been implied as a candidate miRNA biomarker for glaucoma.⁵⁶ With an improved power from cross-trait GWASs, our study suggests *MIR4724* as a potential risk gene underlying UL and BC.

By applying a comprehensive bidirectional MR design, we identified a potential causal relationship between genetic liability to UL and risk of BC, restricted to ER+ subtype. This was largely in line with our genetic correlation analysis on a negligible intrinsic relationship between UL and ER- BC. The strengths of our MR design include (1) genetic instruments derived from the hitherto largest GWAS based on hundreds of thousands of female participants for each trait, (2) reverse-direction MR clarifying the direction of the UL-BC relationship, (3) adjustment for obesity with multi-variable MR to understand the direct effect, and (4) the use of a variety of MR sensitivity analyses to guarantee model assumptions. Consequently, the estimated causal effects were directionally consistent across different statistical approaches and sensitivity analyses, supporting the validity of our findings. Our results are largely concordant with findings from previous case-control studies reporting positive associations of UL and BC^{6,57,58} and a finding from a prospective cohort study that women with a history of UL are at an elevated risk of reporting BC in the future.⁸ While biological mechanisms underlying the observed causal effect remain inconclusive, one might lie in the vertical pleiotropy (or “type II pleiotropy”),⁵⁹ where genetic instruments for UL are associated with other traits (e.g., hormonal response), reflecting the downstream effects of UL that are potentially on the causal pathway linking UL to BC. Findings from our MR analysis have provided genetic evidence for the UL-BC association, highlighting a potential consideration of targeting women with UL for BC prevention (e.g., screening). Future efforts should be focused on the molecular characteristics of UL as well as its clinical factors (e.g., location, multiplicity, size, and recurrence) to target more precisely a population at risk for BC.^{60,61}

Leveraging information on gene expression, we found largely consistent patterns of cell-type-specific heritability enrichment for UL and BC at multiple annotations including the cardiovascular system. Of note, GTEx tissue enrichment analysis also found a cardiovascular component, heart left ventricle, to be significantly enriched by UL-BC shared genes. UL was previously reported to be associated with hypertension and atherosclerosis.^{62,63} A recent prospective study found that, although the presence of UL was not associated with subsequent cardiovascular disease (CVD), risk factors for CVD (particularly BMI and hypertension) were substantially more prevalent in women with UL than in UL-free referents.⁶⁴ It has also been recognized that BC and CVD share a number of common risk factors. Studies have recommended that early recognition and management of CVD risk factors are of utmost importance for BC treatment and prevention.^{65,66} Findings in

our functional annotation analysis suggest possible common pathways leading to the comorbidity between UL and BC, which requires additional work to reveal the underlying pathophysiological mechanism.

As a subtype that possesses neither estrogen nor progesterone receptor (PR),⁶⁷ ER- BC has been considered as less likely to be associated with UL (a hormone-responsive disorder) from a traditional perspective. Using information from genetic data, the current study identified multiple risk loci shared by UL and ER- BC, supporting a non-negligible pleiotropic effect. The similar enrichment patterns regarding the heritability for UL and ER- BC observed at various cell-type-specific annotations further corroborate potential common underlying etiology. Although no evidence on a significant genetic correlation or causal link was shown, it should be noted that the estimated global r_g between UL and ER- BC is similar to that of the ER+ BC ($r_g = 0.06$), with the number of ER- cases being less than a third of their ER+ counterparts. In fact, the significant genetic findings for ER- subtype are not entirely unexpected, as a substantial genetic correlation ($r_g = 0.60$) between the two BC subtypes has already been uncovered by a recent large-scale GWAS.⁶⁸

We acknowledge potential limitations of our study. First, to avoid bias from population stratification, all genetic data in this study were restricted to European ancestry, limiting the generalizability to other ethnic populations. Second, as most of the analytical software adopted by us do not currently support the management and analysis of sex chromosomes, we included only data from autosomes in our study (except in the MR analysis). This may lead to potentially undetected associations due to underrepresentation of X chromosome SNPs. Third, statistical power might be insufficient for the ER- subgroup, yielding null findings which might have been discovered with a larger sample size. Similarly, additional BC subtypes based on other hormonal receptor expression such as PR and human epidermal growth factor receptor 2 (HER2)⁶⁹ were not investigated in this study due to limited sample size, for instance, the HER2 enriched-like BC cases analyzed by Zhang et al.¹¹ ($n = 2,884$). Future studies with larger sample sizes of subtype-specific BC are warranted to extend our findings. Finally, we used limited numbers of UL-associated SNPs as IVs to detect the causal effect of UL on BC, making it difficult to rule out weak instrument bias. However, each SNP-exposure association had an F -statistic greater than 10, supporting the strength of the genetic variants. We emphasize that our inferred causal relationship is putative as it was generated based on GWAS summary statistics. Larger and more powerful GWASs for UL and BC are needed to establish definitively (or rule out) a potential causal link. Future longitudinal studies as well as experimental work are also warranted to investigate the biological mechanism underlying the observed genetic relationship.

To conclude, the current study furthers our understanding to the observational association between UL and BC by

providing evidence of genetic correlation, revealing potential pleiotropic loci, and inferring a putative causal relationship. Our findings highlight an intrinsic link underlying these two complex female diseases and shed new light on the biological mechanisms; these findings might provide important directions for future therapeutic strategy as well as risk prediction.

Data and code availability

This study did not generate datasets or code.

Supplemental information

Supplemental information can be found online at <https://doi.org/10.1016/j.ajhg.2022.05.015>.

Acknowledgments

Summary statistics for the genetic associations with uterine leiomyoma, breast cancer overall, and breast cancer subtypes were obtained from GWASs conducted by Gallagher et al., Zhang et al., and Michailidou et al. We are grateful to all investigators who shared genome-wide summary statistics. This work was supported by funds from the National Natural Science Foundation of China (No. 81874282), the National Key R&D Program of China (2020YFC2006505), the Health Commission of Sichuan Province (20PJ093), and the U.S. National Institutes of Health/Eunice Kennedy Shriver National Institute of Child Health and Human Development (HD060530). Graphical abstract was created with [BioRender.com](https://www.biorender.com).

Declaration of interests

The authors declare no competing interests.

Received: February 17, 2022

Accepted: May 25, 2022

Published: July 7, 2022

Web resources

23andMe GWAS summary statistics, <https://research.23andme.com/dataset-access/>
3DSNP, <http://cbportal.org/3dsnp/>
Coloc, <https://chr1swallace.github.io/coloc/>
CPASSOC, <http://hal.case.edu/~xxz10/zhuweb/>
FM-summary, <https://github.com/hailianghuang/FM-summary>
FUMA, <https://fuma.ctglab.nl/>
GWAS summary statistics for BC overall and subtype-specific BC, <https://bcac.ccge.medschl.cam.ac.uk/bcacdata/oncoarray/oncoarray-and-combined-summary-result/LDSC>, <https://github.com/bulik/ldsc>
NHGRI-EBI GWAS Catalog: UL GWAS summary statistics (without 23andMe), <https://www.ebi.ac.uk/gwas/downloads/summary-statistics>
PLINK, <https://www.cog-genomics.org/plink/1.9/>
 ρ -HESS, https://huwenboshi.github.io/hess/local_rho/
TwoSampleMR, <https://mrcieu.github.io/TwoSampleMR/>

VEP, <https://grch37.ensembl.org/info/docs/tools/vep/index.html>

Webgestalt, <http://webgestalt.org>

References

1. Stewart, E.A., Cookson, C.L., Gandolfo, R.A., and Schulze-Rath, R. (2017). Epidemiology of uterine fibroids: a systematic review. *BJOG* 124, 1501–1512. <https://doi.org/10.1111/1471-0528.14640>.
2. Marino, J.L., Eskenazi, B., Warner, M., Samuels, S., Vercellini, P., Gavoni, N., and Olive, D. (2004). Uterine leiomyoma and menstrual cycle characteristics in a population-based cohort study. *Hum Reprod.* 19, 2350–2355. <https://doi.org/10.1093/HUMREP/DEH407>.
3. Sung, H., Ferlay, J., Siegel, R.L., Laversanne, M., Soerjomataram, I., Jemal, A., and Bray, F. (2021). Global cancer statistics 2020: GLOBOCAN estimates of incidence and mortality Worldwide for 36 cancers in 185 Countries. *CA Cancer J Clin* 71, 209–249. <https://doi.org/10.3322/CAAC.21660>.
4. Pavone, D., Clemenza, S., Sorbi, F., Fambrini, M., and Petraglia, F. (2018). Epidemiology and risk factors of uterine fibroids. *Best Pract. Res. Clin. Obstet. Gynaecol.* 46, 3–11. <https://doi.org/10.1016/j.bpobgyn.2017.09.004>.
5. Shah, R., Rosso, K., and Nathanson, S.D. (2014). Pathogenesis, prevention, diagnosis and treatment of breast cancer. *World J. Clin. Oncol.* 5, 283. <https://doi.org/10.5306/WJCO.V5.I3.283>.
6. Lindegård, B. (1990). Breast cancer among women from Gothenburg with regard to age, mortality and coexisting benign breast disease or leiomyoma uteri. *Oncology* 47, 369–375. <https://doi.org/10.1159/000226850>.
7. Wise, L.A., Radin, R.G., Rosenberg, L., Adams-Campbell, L., and Palmer, J.R. (2015). History of uterine leiomyomata and incidence of breast cancer. *Cancer Causes Control* 26, 1487–1493. <https://doi.org/10.1007/S10552-015-0647-8>.
8. Shen, T.-C., Hsia, T.C., Hsiao, C.L., Lin, C.L., Yang, C.Y., Soh, K.S., Liu, L.C., Chang, W.S., Tsai, C.W., and Bau, D.T. (2017). Patients with uterine leiomyoma exhibit a high incidence but low mortality rate for breast cancer. *Oncotarget* 8, 33014–33023. <https://doi.org/10.18632/ONCOTARGET.16520>.
9. Zhu, Z., Hasegawa, K., Camargo, C.A., and Liang, L. (2021). Investigating asthma heterogeneity through shared and distinct genetics: insights from genome-wide cross-trait analysis. *J. Allergy Clin. Immunol.* 147, 796–807. <https://doi.org/10.1016/J.JACI.2020.07.004>.
10. Gallagher, C.S., Mäkinen, N., Harris, H.R., Rahmioglu, N., Uimari, O., Cook, J.P., Shigeshi, N., Ferreira, T., Velez-Edwards, D.R., Edwards, T.L., et al. (2019). Genome-wide association and epidemiological analyses reveal common genetic origins between uterine leiomyomata and endometriosis. *Nat. Commun.* 10, 4857. <https://doi.org/10.1038/s41467-019-12536-4>.
11. Zhang, H., Ahearn, T.U., Lecarpentier, J., Barnes, D., Beesley, J., Qi, G., Jiang, X., O'Mara, T.A., Zhao, N., Bolla, M.K., et al. (2020). Genome-wide association study identifies 32 novel breast cancer susceptibility loci from overall and subtype-specific analyses. *Nat. Genet.* 52, 572–581. <https://doi.org/10.1038/s41588-020-0609-2>.
12. Rafnar, T., Gunnarsson, B., Stefansson, O.A., Sulem, P., Ingason, A., Frigge, M.L., Stefansdottir, L., Sigurdsson, J.K., Tragante, V., Steinthorsdottir, V., et al. (2018). Variants associating with uterine leiomyoma highlight genetic background shared

- by various cancers and hormone-related traits. *Nat. Commun.* 9, 3636. <https://doi.org/10.1038/S41467-018-05428-6>.
13. Michailidou, K., Lindström, S., Dennis, J., Beesley, J., Hui, S., Kar, S., Lemaçon, A., Soucy, P., Glubb, D., Rostamianfar, A., et al. (2017). Association analysis identifies 65 new breast cancer risk loci. *Nature* 551, 92–94. <https://doi.org/10.1038/nature24284>.
 14. Bulik-Sullivan, B., Finucane, H.K., Anttila, V., Gusev, A., Day, F.R., Loh, P.R., Duncan, L., Perry, J.R.B., Patterson, N., Robinson, E.B., et al. (2015). An atlas of genetic correlations across human diseases and traits. *Nat. Genet.* 47, 1236–1241. <https://doi.org/10.1038/ng.3406>.
 15. Shi, H., Mancuso, N., Spendlove, S., and Pasaniuc, B. (2017). Local genetic correlation gives insights into the shared genetic architecture of complex traits. *Am. J. Hum. Genet.* 101, 737–751. <https://doi.org/10.1016/j.ajhg.2017.09.022>.
 16. Finucane, H.K., Bulik-Sullivan, B., Gusev, A., Trynka, G., Reshef, Y., Loh, P.R., Anttila, V., Xu, H., Zang, C., Farh, K., et al. (2015). Partitioning heritability by functional annotation using genome-wide association summary statistics. *Nat. Genet.* 47, 1228–1235. <https://doi.org/10.1038/ng.3404>.
 17. Zhu, X., Feng, T., Tayo, B., Liang, J., Young, J., Franceschini, N., Smith, J., Yanek, L., Sun, Y., Edwards, T., et al. (2015). Meta-analysis of correlated traits via summary statistics from GWASs with an application in hypertension. *Am. J. Hum. Genet.* 96, 21–36. <https://doi.org/10.1016/j.ajhg.2014.11.011>.
 18. Purcell, S., Neale, B., Todd-Brown, K., Thomas, L., Ferreira, M.A., Bender, D., Maller, J., Sklar, P., de Bakker, P.I., Daly, M.J., and Sham, P.C. (2007). PLINK: a tool set for whole-genome association and population-based linkage analyses. *Am. J. Hum. Genet.* 81, 559–575. <https://doi.org/10.1086/519795>.
 19. Zerbino, D.R., Achuthan, P., Akanni, W., Amode, M., Barrell, D., Bhai, J., Billis, K., Cummins, C., Gall, A., Girón, C.G., et al. (2018). *Nucleic Acids Res.* 46, D754–D761. <https://doi.org/10.1093/NAR/GKX1098>.
 20. Lu, Y., Quan, C., Chen, H., Bo, X., and Zhang, C. (2017). 3DSNP: a database for linking human noncoding SNPs to their three-dimensional interacting genes. *Nucleic Acids Res.* 45, D643–D649. <https://doi.org/10.1093/NAR/GKW1022>.
 21. Schaid, D.J., Chen, W., and Larson, N.B. (2018). From genome-wide associations to candidate causal variants by statistical fine-mapping. *Nat. Rev. Genet.* 19, 491–504. <https://doi.org/10.1038/S41576-018-0016-Z>.
 22. Farh, K.K.-H., Marson, A., Zhu, J., Kleinewietfeld, M., Housley, W.J., Beik, S., Shores, N., Whitton, H., Ryan, R.J.H., Shishkin, A.A., et al. (2014). Genetic and epigenetic fine mapping of causal autoimmune disease variants. *Nature* 518, 337–343. <https://doi.org/10.1038/nature13835>.
 23. Giambartolomei, C., Vukcevic, D., Schadt, E.E., Franke, L., Hingorani, A.D., Wallace, C., and Plagnol, V. (2014). Bayesian test for colocalisation between pairs of genetic association studies using summary statistics. *PLOS Genet.* 10, e1004383. <https://doi.org/10.1371/JOURNAL.PGEN.1004383>.
 24. Zhang, B., Kirov, S., and Snoddy, J. (2005). WebGestalt: an integrated system for exploring gene sets in various biological contexts. *Nucleic Acids Res.* 33, W741–W748. <https://doi.org/10.1093/NAR/GKI475>.
 25. Watanabe, K., Taskesen, E., van Bochoven, A., and Posthuma, D. (2017). Functional mapping and annotation of genetic associations with FUMA. *Nat. Commun.* 8, 1826. <https://doi.org/10.1038/s41467-017-01261-5>.
 26. Finucane, H.K., Reshef, Y.A., Anttila, V., Slowikowski, K., Gusev, A., Byrnes, A., Gazal, S., Loh, P.R., Lareau, C., Shores, N., et al. (2018). Heritability enrichment of specifically expressed genes identifies disease-relevant tissues and cell types. *Nat. Genet.* 50, 621–629. <https://doi.org/10.1038/s41588-018-0081-4>.
 27. Burgess, S., Scott, R.A., Timpson, N.J., Davey Smith, G., and Thompson, S.G. (2015). Using published data in Mendelian randomization: a blueprint for efficient identification of causal risk factors. *Eur. J. Epidemiol.* 30, 543–552. <https://doi.org/10.1007/S10654-015-0011-Z>.
 28. Bowden, J., Davey Smith, G., and Burgess, S. (2015). Mendelian randomization with invalid instruments: effect estimation and bias detection through Egger regression. *Int. J. Epidemiol.* 44, 512–525. <https://doi.org/10.1093/IJE/DYV080>.
 29. Bowden, J., Davey Smith, G., Haycock, P.C., and Burgess, S. (2016). Consistent estimation in mendelian randomization with some invalid instruments using a weighted median estimator. *Genet. Epidemiol.* 40, 304–314. <https://doi.org/10.1002/GEPI.21965>.
 30. Davey Smith, G., and Ebrahim, S. (2003). ‘Mendelian randomization’: can genetic epidemiology contribute to understanding environmental determinants of disease? *Int. J. Epidemiol.* 32, 1–22. <https://doi.org/10.1093/IJE/DYG070>.
 31. Verbanck, M., Chen, C.-Y., Neale, B., and Do, R. (2018). Detection of widespread horizontal pleiotropy in causal relationships inferred from Mendelian randomization between complex traits and diseases. *Nat. Genet.* 50, 693–698. <https://doi.org/10.1038/s41588-018-0099-7>.
 32. Burgess, S., and Thompson, S.G. (2015). Multivariable mendelian randomization: the use of pleiotropic genetic variants to estimate causal effects. *Am. J. Epidemiol.* 181, 251–260. <https://doi.org/10.1093/AJE/KWU283>.
 33. Forouzanfar, N., Baranova, A., Milanizadeh, S., Heravi-Mousavi, A., Jebelli, A., and Abbaszadegan, M.R. (2017). Novel candidate genes may be possible predisposing factors revealed by whole exome sequencing in familial esophageal squamous cell carcinoma. *Tumor Biol.* 39, 101042831769911. <https://doi.org/10.1177/1010428317699115>.
 34. Shinjo, K., Yamashita, Y., Yamamoto, E., Akatsuka, S., Uno, N., Kamiya, A., Niimi, K., Sakaguchi, Y., Nagasaka, T., Takahashi, T., et al. (2014). Expression of chromobox homolog 7 (CBX7) is associated with poor prognosis in ovarian clear cell adenocarcinoma via TRAIL-induced apoptotic pathway regulation. *Int. J. Cancer* 135, 308–318. <https://doi.org/10.1002/IJC.28692>.
 35. Kreis, N.-N., Louwen, F., and Yuan, J. (2019). The multifaceted p21 (Cip1/Waf1/CDKN1A) in cell differentiation, migration and cancer therapy. *Cancers (Basel)* 11, 1220. <https://doi.org/10.3390/CANCERS11091220>.
 36. Kuban-Jankowska, A., Gorska, M., Knap, N., Cappello, F., and Wozniak, M. (2015). Protein tyrosine phosphatases in pathological process. *Front. Biosci.* 20, 4314–4388. <https://doi.org/10.2741/4314>.
 37. Soto-Quintana, O., Zúñiga-González, G., Ramírez-Patiño, R., Ramos-Silva, A., Figuera, L., Carrillo-Moreno, D., Gutiérrez-Hurtado, I., Puebla-Pérez, A., Sánchez-Llamas, B., and Gallegos-Arreola, M. (2015). Association of the GSTM1 null polymorphism with breast cancer in a Mexican population. *Genet. Mol. Res.* 14, 13066–13075. <https://doi.org/10.4238/2015.OCTOBER.26.2>.
 38. Wang, B., Li, D., Rodriguez-Juarez, R., Farfus, A., Storozynsky, Q., Malach, M., Carpenter, E., Filkowski, J., Lykkesfeldt, A.E., and Kovalchuk, O. (2018). A suppressive role of guanine

- nucleotide-binding protein subunit beta-4 inhibited by DNA methylation in the growth of anti-estrogen resistant breast cancer cells. *BMC Cancer* 18, 817. <https://doi.org/10.1186/S12885-018-4711-0>.
39. Wang, C., Xie, X.X., Li, W.J., and Jiang, D.Q. (2019). LncRNA DLEU1/microRNA-300/RAB22A axis regulates migration and invasion of breast cancer cells. *Eur. Rev. Med. Pharmacol. Sci.* 23, 10410–10421. https://doi.org/10.26355/EURREV_201912_19680.
 40. Song, X., Zhang, M., Chen, L., and Lin, Q. (2017). Bioinformatic prediction of possible targets and mechanisms of action of the green tea compound epigallocatechin-3-gallate against breast cancer. *Front. Mol. Biosci.* 4, 43. <https://doi.org/10.3389/FMOLB.2017.00043>.
 41. Dai, W., and Jiang, L. (2019). Dysregulated mitochondrial dynamics and metabolism in obesity, diabetes, and cancer. *Front. Endocrinol. (Lausanne)* 10, 570. <https://doi.org/10.3389/FENDO.2019.00570>.
 42. Zhuang, J., Huo, Q., Yang, F., and Xie, N. (2020). Perspectives on the role of histone modification in breast cancer progression and the advanced technological tools to study epigenetic determinants of metastasis. *Front. Genet.* 11, 603552. <https://doi.org/10.3389/FGENE.2020.603552>.
 43. Elliott, K., and Larsson, E. (2021). Non-coding driver mutations in human cancer. *Nat. Rev. Cancer* 21, 500–509. <https://doi.org/10.1038/s41568-021-00371-z>.
 44. Cuykendall, T.N., Rubin, M.A., and Khurana, E. (2017). Non-coding genetic variation in cancer. *Curr. Opin. Syst. Biol.* 1, 9–15. <https://doi.org/10.1016/J.COISB.2016.12.017>.
 45. Zhu, Z., Anttila, V., Smoller, J.W., and Lee, P.H. (2018). Statistical power and utility of meta-analysis methods for cross-phenotype genome-wide association studies. *PLoS One* 13, e0193256. <https://doi.org/10.1371/JOURNAL.PONE.0193256>.
 46. Sparling, D.P., Griesel, B.A., Weems, J., and Olson, A.L. (2008). GLUT4 enhancer factor (GEF) interacts with MEF2A and HDAC5 to regulate the GLUT4 promoter in adipocytes. *J. Biol. Chem.* 283, 7429–7437. <https://doi.org/10.1074/JBC.M800481200>.
 47. Zhao, Y., Yun, D., Zou, X., Jiang, T., Li, G., Hu, L., Chen, J., Xu, J., Mao, Y., Chen, H., and Lu, D. (2017). Whole exome-wide association study identifies a missense variant in SLC2A4RG associated with glioblastoma risk. *Am. J. Cancer Res.* 7, 1937.
 48. Paul, M.R., Pan, T.C., Pant, D.K., Shih, N.N., Chen, Y., Harvey, K.L., Solomon, A., Lieberman, D., Morrisette, J.J., Soucier-Ernst, D., et al. (2020). Genomic landscape of metastatic breast cancer identifies preferentially dysregulated pathways and targets. *J. Clin. Invest.* 130, 4252–4265. <https://doi.org/10.1172/JCI129941>.
 49. Sallusto, F. (2013). DCs: a dual bridge to protective immunity. *Nat. Immunol.* 14, 890–891. <https://doi.org/10.1038/ni.2693>.
 50. Fararjeh, A.S., and Liu, Y.N. (2019). ZBTB46, SPDEF, and ETV6: novel potential biomarkers and therapeutic targets in castration-resistant prostate cancer. *Int. J. Mol. Sci.* 20, 2802. <https://doi.org/10.3390/IJMS20112802>.
 51. Chen, W.Y., Tsai, Y.C., Siu, M.K., Yeh, H.L., Chen, C.L., Yin, J.J., Huang, J., and Liu, Y.N. (2017). Inhibition of the androgen receptor induces a novel tumor promoter, ZBTB46, for prostate cancer metastasis. *Oncogene* 36, 6213–6224. <https://doi.org/10.1038/ONC.2017.226>.
 52. Xu, N., Wang, F., Lv, M., and Cheng, L. (2015). Microarray expression profile analysis of long non-coding RNAs in human breast cancer: a study of Chinese women. *Biomed. Pharmacother.* 69, 221–227. <https://doi.org/10.1016/J.BIOPHA.2014.12.002>.
 53. Pertesi, M., Ekdahl, L., Palm, A., Johnsson, E., Järnvstråt, L., Wihlborg, A.K., and Nilsson, B. (2019). Essential genes shape cancer genomes through linear limitation of homozygous deletions. *Commun. Biol.* 2, 262. <https://doi.org/10.1038/s42003-019-0517-0>.
 54. Yu, Y.-H., Xin, F., Dong, L., Ge, L., Zhai, C.-Y., and Shen, X.-L. (2020). Weighted Gene Coexpression Network Analysis Identifies Critical Genes in Different Subtypes of Acute Myeloid Leukaemia. *Biotechnol. Biotechnol. Equipment* 34, 925–936. <https://doi.org/10.1080/13102818.2020.1811767>.
 55. Jeffrey, S.S. (2008). Cancer biomarker profiling with microRNAs. *Nat. Biotechnol.* 26, 400–401. <https://doi.org/10.1038/nbt0408-400>.
 56. Hindle, A.G., Thoonen, R., Jasien, J.V., Grange, R.M.H., Amin, K., Wise, J., Ozaki, M., Ritch, R., Malhotra, R., and Buys, E.S. (2019). Identification of candidate miRNA biomarkers for Glaucoma. *Invest Ophthalmol. Vis. Sci.* 60, 134. <https://doi.org/10.1167/IOVS.18-24878>.
 57. Tseng, J.J., Chen, Y.H., Chiang, H.Y., and Lin, C.H. (2017). Increased risk of breast cancer in women with uterine myoma: a nationwide, population-based, case-control study. *J. Gynecol. Oncol.* 28, e35. <https://doi.org/10.3802/JGO.2017.28.E35>.
 58. Chuang, S.-C., Wu, G.-J., Lu, Y.-S., Lin, C.-H., and Hsiung, C.A. (2015). Associations between medical Conditions and breast cancer risk in Asians: a nationwide population-based study in Taiwan. *PLoS One* 10, e0143410. <https://doi.org/10.1371/JOURNAL.PONE.0143410>.
 59. Davey Smith, G., and Hemani, G. (2014). Mendelian randomization: genetic anchors for causal inference in epidemiological studies. *Hum. Mol. Genet.* 23, R89–R98. <https://doi.org/10.1093/HMG/DDU328>.
 60. Sakai, K., Tanikawa, C., Hirasawa, A., Chiyoda, T., Yamagami, W., Kataoka, F., Susumu, N., Terao, C., Kamatani, Y., Takahashi, A., et al. (2020). Identification of a novel uterine leiomyoma GWAS locus in a Japanese population. *Sci. Rep.* 10, 1197. <https://doi.org/10.1038/s41598-020-58066-8>.
 61. Dvorská, D., Braný, D., Danková, Z., Danková, Z., Halašová, E., Halašová, E., Višňovský, J., and Višňovský, J. (2017). Molecular and clinical attributes of uterine leiomyomas. *Tumor Biol.* 39, 101042831771022. <https://doi.org/10.1177/1010428317710226>.
 62. Aksoy, Y., Sivri, N., Karaoz, B., Sayin, C., and Yetkin, E. (2014). Carotid intima-media thickness: a new marker of patients with uterine leiomyoma. *Eur. J. Obstet. Gynecol. Reprod. Biol.* 175, 54–57. <https://doi.org/10.1016/J.EJOGRB.2014.01.005>.
 63. Boynton-Jarrett, R., Rich-Edwards, J., Malspeis, S., Missmer, S.A., and Wright, R. (2005). A prospective study of hypertension and risk of uterine leiomyomata. *Am. J. Epidemiol.* 161, 628–638. <https://doi.org/10.1093/AJE/KW1072>.
 64. Laughlin-Tommaso, S.K., Fuchs, E.L., Wellons, M.F., Lewis, C.E., Calderon-Margalit, R., Stewart, E.A., and Schreiner, P.J. (2019). Uterine fibroids and the risk of cardiovascular disease in the coronary artery risk development in young adult women's study. *J. Women's Heal.* 28, 46–52. <https://doi.org/10.1089/JWH.2018.7122>.
 65. Mehta, L.S., Watson, K.E., Barac, A., Beckie, T.M., Bittner, V., Cruz-Flores, S., Dent, S., Kondapalli, L., Ky, B., Okwuosa, T., et al. (2018). Cardiovascular disease and breast cancer: where these entities intersect: a scientific statement from the

- American heart association. *Circulation* 137, e30–e66. <https://doi.org/10.1161/CIR.0000000000000556>.
66. Almuwaqqat, Z., Meisel, J.L., Barac, A., and Parashar, S. (2019). Breast cancer and heart failure. *Heart Fail Clin.* 15, 65–75. <https://doi.org/10.1016/j.hfc.2018.08.007>.
67. Althuis, M.D., Fergenbaum, J.H., Garcia-Closas, M., Brinton, L.A., Madigan, M.P., and Sherman, M.E. (2004). Etiology of hormone receptor-defined breast cancer: a systematic review of the literature. *Cancer Epidemiol. Biomarkers Prev.* 13, 1558–1568. <https://pubmed.ncbi.nlm.nih.gov/15466970/>.
68. Milne, R.L., Kuchenbaecker, K.B., Michailidou, K., Beesley, J., Kar, S., Lindström, S., Hui, S., Lemaçon, A., Soucy, P., Dennis, J., et al. (2017). Identification of ten variants associated with risk of estrogen-receptor-negative breast cancer. *Nat. Genet.* 49, 1767–1778. <https://doi.org/10.1038/NG.3785>.
69. Onitilo, A.A., Engel, J.M., Greenlee, R.T., and Mukesh, B.N. (2009). Breast cancer subtypes based on ER/PR and Her2 expression: comparison of clinicopathologic features and survival. *Clin Med Res* 7, 4–13. <https://doi.org/10.3121/cm.2008.825>.